A&A 388, 74–87 (2002)
DOI: 10.1051/0004-6361:20020435

Astronomy & Astrophysics

XMM–Newton observations of the Seyfert 1 galaxy Mrk 335

P. Gondoin, A. Orr, D. Lumb, and M. Santos-Lleo

Research and Scientific Support Department, European Space Agency – Postbus 299, 2200 AG Noordwijk, The Netherlands

Received 18 January 2002 / Accepted 21 March 2002

Abstract. We report on an *XMM–Newton* observation of the Seyfert 1 galaxy Mrk 335 performed in December 2000. The power law component of its spectrum above 2 keV has a photon index $\Gamma = 2.3$ much steeper than that of a "normal" Seyfert 1 galaxy. A broad spectral feature is observed around 6.0 keV (± 1 keV) that can be fitted by a relativistic emission profile or by an edge. A soft excess above the power law rises steeply below 2 keV and represents more than 30% of the intrinsic source luminosity in the 0.3–2 keV band. Large luminosity ($\Delta L > 5 \times 10^{42}$ erg s^{-1}) variations on time scales of a few ksec support the view that gravitational energy conversion linked with the presence of a supermassive object is likely responsible for the X-ray emission from Mrk 335 nucleus. The relativistic line profile points to a scenario where the iron K emission arises from highly ionized material in the innermost region of an accretion disk surrounding a rotating black hole. The soft excess emission partly results from reprocessing onto the highly ionized inner region of the disk of a power law continuum produced by inverse Compton scattering of UV photons within a corona above the disk. Thermal emission produced by the viscous heating of the disk itself could also contribute to the soft excess emission in Mrk 335. We argue that, within the innermost region of the disk, the dynamics of accretion could become similar to spherical accretion and advection-dominated with a radiation efficiency as low as 0.25%. A rate of accretion constrained to 13% of the Eddington limit onto a central 10^7 $M_\odot$ object would then translate into 1.6×10^{-2} $M_\odot$ yr^{-1}. We further conjecture that Mrk 335 might be in a transition between a normal Seyfert 1 state and an ultra-soft NLS1 state where the soft-excess emission would be fully dominated by the intrinsic emission from the accreting material.

Key words. galaxies: individual: Mrk 335 – galaxies: nuclei – galaxies: Seyfert

1. Introduction

Mrk 335 is a nearby Seyfert 1 galaxy at a redshift $z = 0.026$, first detected in X-rays by *UHURU* (Tananbaum et al. 1978). Subsequent *EXOSAT* observations (Pounds et al. 1987) established the existence of a two-component X-ray spectrum in the 0.1–10 keV band, including a steep spectral component dominating the soft X-ray spectrum, and an unusually strong variability on timescales of 1–2 hr. These X-ray spectral properties are a characteristic of narrow-line Seyfert 1 (NLS1) galaxies which show very steep spectra due to a significant soft excess in the 0.1–2.4 keV X-ray band (Boller et al. 1996). Indeed, Mrk 335 is often classified as a NLS1 galaxy but has a relatively large Hβ *FWHM* (1640 km s^{-1}, Wang et al. 1996), close to the 2000 km s^{-1} boundary which conventionally separates narrow-line from broad-line Seyfert 1 galaxies. The extreme X-ray properties of NLS1 galaxies make them ideal objects for understanding many of the physical processes occuring within the active nuclei of Seyfert galaxies.

The spectrum of Mrk 335 exhibits a prominent big blue bump. Based on observations in the UV, optical and infrared bands, Edelson & Malkan (1986) and Sun & Malkan (1989) construct a spectrum with a notable UV excess, which can be fitted with a blackbody at 25 600 K. Pounds et al. (1987) suggest that the strong soft excess, which was observed with EXOSAT and later on with ROSAT (Turner et al. 1993) and Ginga (Nandra & Pounds 1994), could be the high energy tail of the accretion disk spectrum. Zheng et al. (1995) find that an accretion disk spectrum with a Lyman edge feature provides a good match to the UV and optical continuum of Mrk 335. Both a disk emitting as a blackbody and a disk Comptonized by a hot corona, provide equally good descriptions of the observed UV continuum shape. However, only the Comptonized disk has a sufficiently hard X-ray spectrum to match the observed soft X-ray excess.

A significant fraction of type 1 active galactic nuclei (Reynolds 1997) show K-shells absorption edges of warm oxygen (O VII and O VIII) characteristic of optically thin, photoionized material along the line of sight to the central engine, the so-called warm absorber. No clear evidence for warm absorption is present in *ASCA* data of Mrk 335 (Reynolds 1997; George et al. 1998; Leighly 1999). Recently, Ballantyne et al. (2001) have found that a good fit to the *ASCA* spectrum of Mrk 335 is achieved with a ionized disc model (Ross & Fabian 1993). Simulations of spectra resulting from such a model have been performed

Send offprint requests to: P. Gondoin,
e-mail: pgondoin@rssd.esa.int

by Ross et al. (1999) for a wide range of ionization parameters assuming uniform density slabs of gas illuminated by a power law spectrum. For soft X-rays ($E < 1.5$ keV), results indicate that reflection effects of the primary continuum can be greatly enhanced owing to Bremsstrahlung emission by the hot surface layer and "inverse Compton" upscattering of even softer photons. As the lighter elements become partly ionized in the deeper layers, line emission at soft X-ray energies would become important (Ross & Fabian 1993; Zycki et al. 1994). Partially ionized iron could also give rise to emission above the 6.4 keV fluorescence line from neutral material, which could explain why *ASCA* (Reynolds 1997) detected a strong iron Kα line in the spectrum of Mrk 335.

In this paper, we report the analysis results of *XMM–Newton* observations of Mrk 335 performed in December 2000. Section 2 details the observations and data reduction procedures. Section 3 presents the integrated flux measurements and their temporal behaviour during the observations. Sections 4 and 5 describe the spectral analysis which was performed in two steps including first a characterization of the Fe K spectral features around 6.4 keV and then an analysis of the entire 0.3−10 keV energy range. The analysis results are discussed in Sect. 6.

2. Observations and data reduction

Mrk 335 was observed by the *XMM–Newton* space observatory (Jansen et al. 2001) between 2000 December 25 16:24:04 (UT) and 2000 December 26 02:45:11 (UT) for usable exposure times of 32.1 ksec (EPIC p−n camera), 34.2 ksec (EPIC MOS 1 and MOS 2 cameras) and 36.9 ksec (RGS 1 and RGS 2 reflection grating spectrometers). *XMM–Newton* uses three grazing incidence telescopes which provide an effective area >4000 cm^2 at 2 keV and 1600 cm^2 at 8 keV (Gondoin et al. 2000). Three EPIC CCD cameras (Strüder et al. 2001; Turner et al. 2001) at the prime focus of the telescopes provide imaging in a 30′ field of view and broadband spectroscopy with a resolving power of between 5 and 60 in the energy range 0.3 to 10 keV. Two identical RGS reflection grating spectrometers behind two of the X-ray telescopes allow high resolution ($E/\Delta E = 100$ to 500) measurements in the soft X-ray range (6 to 38 Å or 0.3 to 2.1 keV) with a maximum effective area of about 140 cm^2 at 15 Å (den Herder et al. 2001).

The observations of Mrk 335 were conducted with the EPIC p−n camera operating in full frame mode and with the EPIC MOS cameras operating in large window mode. RGS spectra were recorded simultaneously. "Medium" thickness aluminum filters were used in front of all CCD cameras to reject visible light. The raw event data sets were processed with the "emproc", "epproc" and "rgsproc" pipeline tasks of the *XMM–Newton* Science Analysis System (SAS version 5.2.0) in order to generate calibrated event lists. The large count rate of the target produced pile-up effects in the core of the telescope point spread functions registered by the EPIC cameras. In order to reject these ambiguous events, the source spectra in the EPIC MOS cameras were built from photons detected within an annulus of radius included between 10″ and 73″ from the target boresight. The background was estimated on the same CCD chips within windows of similar size which were offset by about 2.8′ from the source centroid position. The source spectrum in the EPIC pn cameras was built from photons detected within an annulus of radius included between 10″ and 54″ from the target boresight. Background rates were found to be extremely low during the whole observation. The Pulse-Invariant (PI) spectra were rebinned such that each resultant channel had at least 50 counts per bin in the p–n spectra and 25 counts per bin in the MOS spectra. χ^2 minimization was used for the spectral fitting. All such fits were performed using the XSPEC package (v11). The EPIC response matrices were generated using the SAS tasks "rmfgen" and "arfgen" taking into account the annular shape of the source extraction windows. The RGS response matrices were generated by the SAS task "rgsrmfgen".

3. Integrated flux and temporal behaviour

The spectral analysis of the Mrk 335 *XMM–Newton* data (see Sect. 5) yields flux measurements in the low (0.3−2 keV) and high (2−10 keV) energy bands of $F_{\rm LE} = 2.25 \times 10^{-11}$ erg cm^{-2} s^{-1} and $F_{\rm HE} = 0.96 \times 10^{-11}$ erg cm^{-2} s^{-1}, respectively. After correction of the galactic absorption by hydrogen column density ($N_{\rm H} = 4.0 \times 10^{20}$ cm^{-2}), these correspond to luminosities of $L_{\rm LE} = 4.03 \times 10^{43}$ erg s^{-1} and $L_{\rm HE} = 1.24 \times 10^{43}$ ergs s^{-1} for $z = 0.026$ and $H_0 = 75$ km s^{-1} Mpc^{-1}. The derived luminosity in the high energy band is comparable to the 2.3×10^{43} erg s^{-1} value ($H_0 = 50$ km s^{-1} Mpc^{-1}) reported by Bianchi et al. (1999) in the 2–10 keV band from a *BeppoSAX* observation of Mrk 335 performed in December 1999.

A linear regression to the light curves illustrates (see Fig. 1) the increase of the source flux in the low and high energy bands. The EPIC p−n count rates increased by $33 \pm 3\%$ in the 0.3−2 keV spectral range over the 34 ksec observation period. In addition to this steady flux increase, count rates variations of amplitude >5% are detected on time scales as short as a few ksec. The time variability behaviour is identical in the low and high energy band. The X-ray emission varies erratically and is not correlated with any spectral change suggesting that all spectral components originate from the same region. This is illustated in Fig. 2 (top) which shows that the ratio of count rates in the high (HE; 2–10 keV) and low (LE; 0.3–2 keV) energy bands is independent of the source flux. A high variability of Mrk 335 on time scale of hours−days has been previously reported in the literature (Turner & Pounds 1988; Bianchi et al. 1999). The large effective area of the *XMM–Newton* telescopes shows that changes of luminosity $\Delta L > 5 \times 10^{42}$ erg s^{-1} are taking place on size scales

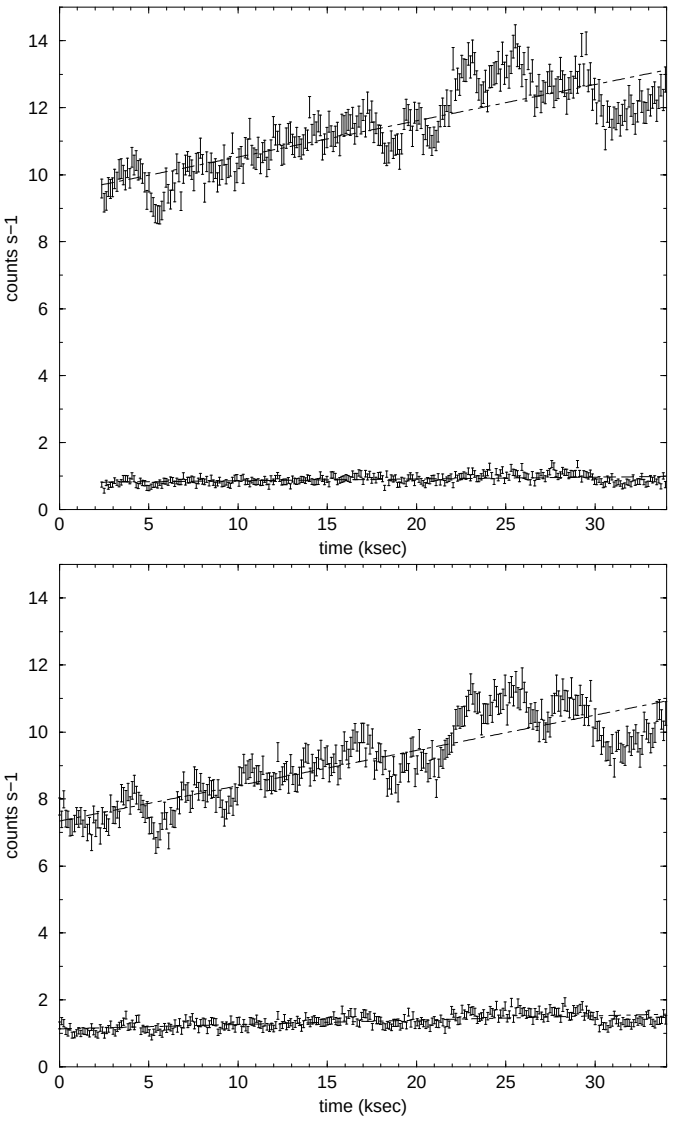

Fig. 1. Light curves of Mrk 335 obtained with the EPIC p−n (top) and the EPIC MOS (bottom) cameras in the 0.3−2 keV (upper curve) and in the 2−10 keV (lower curve) energy bands. The noise rate within the overall band band is negligible. The events are binned into 120 s time intervals. The dot-dashed lines are linear regressions to the light curves.

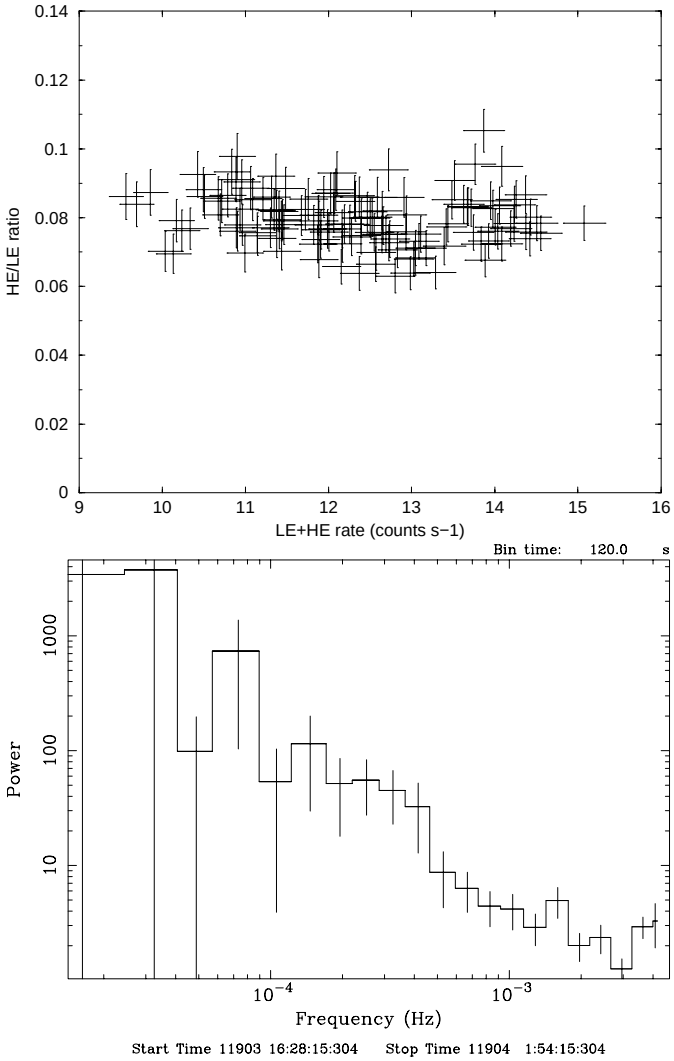

Fig. 2. Top: ratio of EPIC pn count rates in the high (HE; 2–10 keV) and low (LE; 0.3–2 keV) energy bands vs. total count rate. Bottom: power spectral density of EPIC count rates during the 34 ksec observation. The events are binned into 120 s time intervals.

smaller than a light hour, which means that they are associated with a compact phenomenon, only a few AU in size. With the enormous luminosity involved, this result supports the view that gravitational energy conversion linked with the presence of a supermassive object is responsible for the X-ray emission from the nucleus of Mrk 335.

The variance of the luminosity at high frequencies can be estimated by integrating the power spectral density (PSD) of the EPIC count rates obtained during the 34 ksec observation period. The power spectrum of the count rate (see Fig. 2: bottom) looks rather constant on frequencies higher than $\approx 10^{-3}$ Hz and rises steeply below about $4{-}5 \times 10^{-4}$ Hz, thus suggesting a characteristic time scale of about 2 ksec above which the variance of Mrk 335 luminosity suddenly increases. This feature in the PSD of Mrk 335 is reminiscent of a step observed in the X-ray power spectrum of NGC 4051 by Bao & Oostgaard (1994). Within the frame of the current AGN paradigm, these authors interprete this PSD drop-off at high frequencies as an indication of a characteristic time scale related to the presence of a central black hole. Departure from a best fit power-law model (plus a constant Poisson noise level) indicates that this drop-off feature at $4{-}5 \times 10^{-4}$ Hz in the measured power spectrum of MRK 335 is not significant at a 3 σ level. Several changes in luminosity on this timescale can be seen in the light curve (see Fig. 1). During the most dramatic events toward the end of the observation, the 0.3–10 keV flux increased by about 20% ($\approx 10^{43}$ erg s^{-1}) in about 2 ksec. The rate of change in luminosity is in that case $\Delta L/\Delta t \approx 5 \times 10^{39}$ erg s^{-2}.

4. Analysis of the Fe K spectral feature

The main X-ray spectral feature observed in many AGNs is the Fe K fluorescence line at 6.4 keV. A comparison of our Mrk 335 data with a power law model, which best fits the 3–4.5 keV and 8–10 keV spectral bands around the line, shows excess emission at the Fe K line position up to an energy of about 7.0 keV (see Fig. 3) in the observed reference frame. Based on this observation, we initially fit the EPIC data in the high energy range above 2 keV with a phenomenological model consisting of a power law continuum and a Gaussian emission line. The best fit to the EPIC p−n and MOS data gives a rest energy of the line at 6.0 ± 0.14 keV and an equivalent width $EW \approx 996$ eV. If related to an iron Kα fluorescence line, the best fit Gaussian model indicates that the line is broad ($\sigma = 1.2 \pm 0.2$ keV) and redshifted by at least 0.4 keV. An alternative possibility is that the excess emission below 7 keV is in fact the result of an Fe absorption edge imprinted on a less steep power law.

To test the edge hypothesis, we fitted the EPIC data above 2 keV with a power law continuum and an absorption edge. All parameters were left free except the redshift. The best fit model ($\chi^2 = 1.01$) to the EPIC MOS and p−n data indicates an absorption depth $\tau = 0.2 \pm 0.1$ at 7.6 keV ± 0.2 in the source rest frame. Since an absorption edge in Seyfert 1 galaxies is often associated with an emission line (e.g. Gondoin et al. 2001a,b), we added a redshifted Gaussian component to the edge model (see Fig. 2). A line was found at 6.56 ± 0.08 keV in the source rest frame with only a marginal improvement of the fit ($\Delta\chi^2 = -21$ for 611 degrees of freedom). The measured position of the edge at 7.6 ± 0.2 is consistent with a reflection model from optically thick material as detected in this source by Nandra & Pounds (1994). The reflected spectrum is absorbed by iron in low states of ionization up to Fe XVIII. This result contrasts with the possible presence of a narrow Gaussian line at 6.56 ± 0.08 keV which indicates that the iron Fe K emission could mainly arise from material in the highest state of ionization up to Fe XXV. In view of this apparent inconsistency, we considered the emission line model as a likely alternative to the absorption edge model.

Figure 3 shows that the excess emission above the best fit power law to the data in the 3–4.5 keV and 8.0–10 keV spectral ranges extends down to below 5 keV. If due to Fe K emission, the profile of this line is skewed to the low energy end of the spectrum with little emission above 7 keV and significant emission down to 5 keV. Such a shape is expected for lines emitted by accretion disks and modified by relativistic effects (Fabian et al. 1989; Stella 1990). Hence, we fitted the broad emission feature with a DISKLINE (Fabian et al. 1989) and with a LAOR (Laor 1991) model. The DISKLINE model was used with a $(1-(6/R)^{1/2})/R^3$ emissivity law. The LAOR model was tested with two values $\beta = 2$ and 3 for a power law dependence $R^{-\beta}$ of the emissivity. The disk inclination was fixed to 30° in both cases. The inner and outer radii of the relativistic accretion disk are poorly constrained by the DISKLINE model. The LAOR model provides an acceptable fit to the data for both values of β (see Table 1). This suggests that the fluxes which emerge in the extreme red wing of the iron line might be due to the large gravitational redshift experienced by photons from a region of the accretion disk close to the zone of marginal stability. This zone can extend down to 1.2 GM/c^2 for a Kerr black hole spinning at the extreme rate. Furthermore, the LAOR model gives a best fit energy of 7.2 ± 0.2 keV for $\beta = 2$, thus suggesting that iron could be in high states of ionization, up to Fe XXVI. The best fit parameters for the Mrk 335 Fe K line using a relativistic disk line

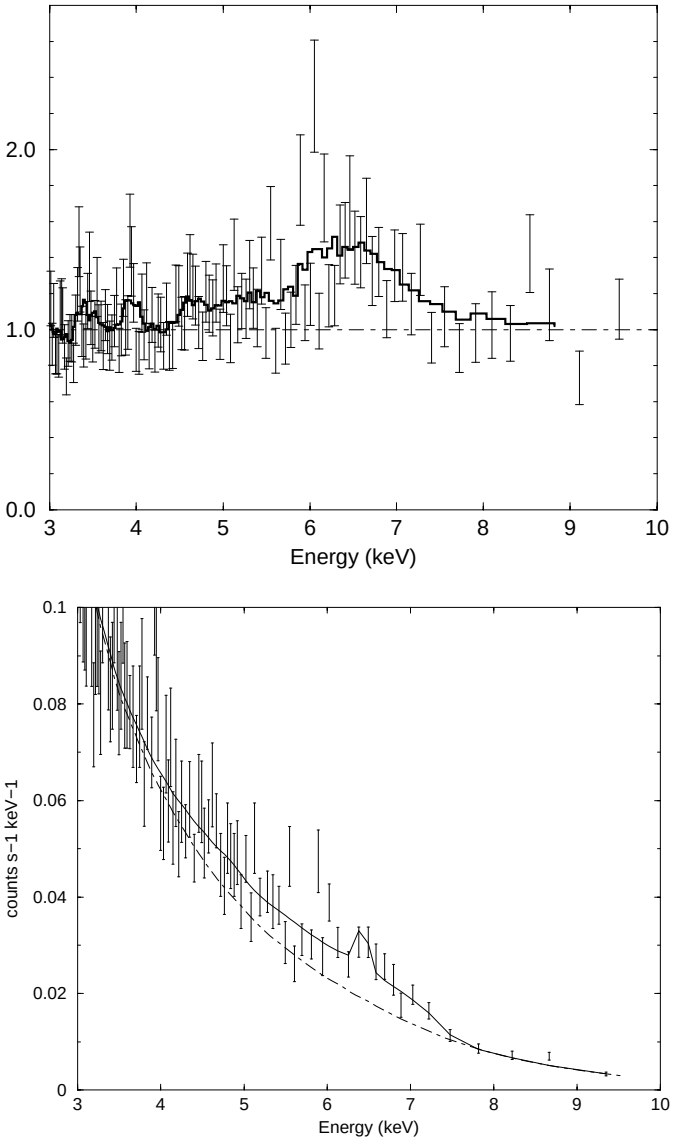

Fig. 3. Top: ratio between the EPIC p−n data and a power law parametrization of the measured continuum (see Table 2). Bottom: comparison of EPIC p−n data with a phenomenological model consisting of a relativistic accretion disk profile (see Table 1) and a narrow Gaussian emission component. The dot-dashed line is the best fit power law to the data in the 3–4.5 keV and 8–10 keV spectral band.

Table 1. Best fit parameters to the EPIC Fe K line spectrum of Mrk 335 assuming emission from a relativistic accretion disc described by the DISKLINE model and by the LAOR model with a power law emissivity ($R^{-\beta}$).

Model parameters	LAOR ($\beta = 2$)	LAOR ($\beta = 3$)	DISKLINE
Line energy (keV)	6.97 (frozen)	6.97 (frozen)	6.97 (frozen)
Line equivalent width (keV)	0.966	0.849	0.834
Inner radius (units of GM/c^2)	4.0 ± 0.5	4.1 ± 0.3	6.0 ± 9.0
Outer radius (units of GM/c^2)	11.5 ± 1.2	12.4 ± 1.9	8.0 ± 0.5
Disk inclination ($^\circ$)	30 (frozen)	30 (frozen)	30 (frozen)
Line norm. (ph cm^{-2} s^{-1})	$3.4 \pm 0.8 \times 10^{-5}$	$3.6 \pm 0.8 \times 10^{-5}$	$3.0 \pm 0.7 \times 10^{-5}$
χ^2_ν	352/354	352/354	369/354

profile therefore point to a scenario where the iron K emission arises from highly ionized material in the innermost region of an accretion disk surrounding a rotating black hole. Table 1 lists the best fit parameters to the Mrk 335 Fe K line profile with a rest-frame line energy fixed at 6.97 keV.

In order to assess the presence of an other component that could arise from iron in lower ionisation states, we added a narrow Gaussian line to the broad LAOR profile (see Fig. 3). A best fit rest energy of the narrow line is found at 6.6 ± 0.4 keV. This value is suggestive of emission from iron in a high Fe XXV ionization state but the improvement of the fit with this additional component is not significant ($\Delta\chi^2 = -4$ for 354 degrees of freedom).

5. Analysis of the continuum emission

5.1. Phenomenological model

In order to characterize the continuum emission of Mrk 335 spectrum, we extended the analysis of EPIC data to the 0.3–10 keV energy range. Comparisons of the spectra with the best fit power law model established above 2 keV show large residuals at soft energies. This led us to add a soft excess component to the power law model. We tested a blackbody, a Bremsstrahlung and a second power law component. The two component models were combined with neutral galactic absorption using the cross-sections of Morrison & McCammon (1983) assuming galactic absorption with solar abundance and $N_{\rm H} = 4.0 \times 10^{20}$ cm^{-2} (Stark et al. 1992). The power law and the blackbody models give an unacceptable fit to the soft excess-emission both for the MOS and p−n data, with a reduced χ^2 of respectively 1.35 and 1.30. The redshifted power law + thermal Bremsstrahlung model provides a good description of the spectra (see Table 2). We find a Bremsstrahlung temperature $kT = 0.27 \pm 0.01$ keV and a power law index $\Gamma = 2.29 \pm 0.02$ (see Fig. 4). The Bremsstrahlung model for this temperature regime is regarded as a parametrization of the source continuum emission at soft energies and not as a physically consistent model. The integrated Bremstrahlung emission over the 0.3 to 2 keV spectral band measures the soft excess emission above the power law. It represents ≈32% of the intrinsic source flux in that band after correction for Galactic absorption.

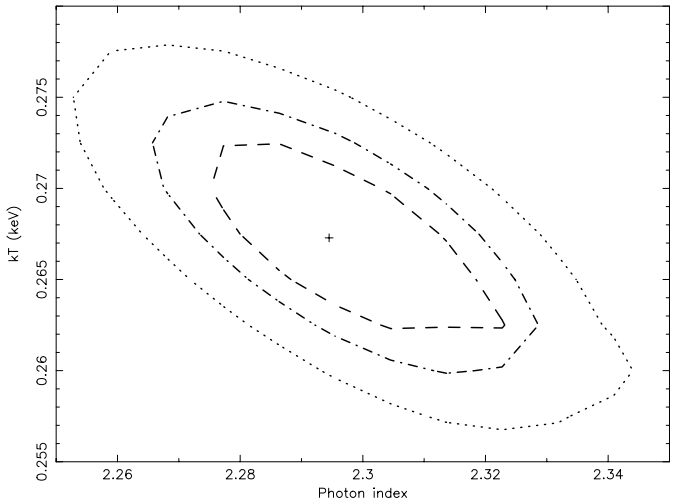

Fig. 4. EPIC confidence contours (corresponding to 68, 90 and 95 percent confidence levels) for Bremstrahlung temperature versus the photon index of the power law.

5.2. Reflection from moderately ionized material

Our analysis of the Fe K line in Mrk 335 suggests that the X-ray emission could arise from ionized material in the inner region of an accretion disk. Evidence for ionized accretion discs have been found in NLS1 galaxies (TON S 180: Comastri et al. 1998; Turner et al. 1998; Ark 564: Vaughan et al. 1999). These conclusions are based on either the energy centroid of the observed Fe Kα line or on spectral fits using the PEXRIV ionized disc model of Magdziarz & Zdziarski (1995). Ionized reflection has observable effects over the whole X-ray continuum, so tighter constraints on the ionization state can be obtained by fitting the ionized disc model over the entire observed energy range. Hence, we replace the power law + Bremstrahlung continuum by the PEXRIV reflection model from ionized material. Since, in PEXRIV, the relativistic smearing is not applied to the reflection continuum, we also tested the REFSCH+DISKLINE model. In this model, an exponentially cut-off power-law spectrum reflected from an ionized relativistic accretion disk (Magdziarz & Zdziarski 1995) is convolved with a relativistic disk line profile. The REFSCH+DISKLINE model does not give an acceptable fit to the data. The PEXRIV+LAOR model alone gives a marginally acceptable fit with a reduced χ^2 of 1.2 but with an unphysically high reflection fraction. Hence, we

Table 2. Best fit parametrization of the measured continuum emission.

Model component	Parameters	
WABS	$N_{\rm H}$ (cm^{-2})	4.0×10^{20}
ZBREMSS	kT (keV)	0.27 ± 0.01
	Norm.	$1.99 \times 10^{-2} \pm 0.24 \times 10^{-2}$
ZPOWERLW	Γ	2.29 ± 0.02
	Norm. (ph keV^{-1} cm^{-2} s^{-1})	$2.6 \pm 0.4 \times 10^{-3}$
	χ^2_ν	1.12

Table 3. Spectral fits with ionized reflection models and soft excess. The ionization parameter ξ is calculated either in the 0.01–100 keV band (RF model) or in the 5–20 keV band (PEXRIV model). A comparison between these models requires the multiplication of the ionization parameter by a conversion factor $\xi_{\rm RF}/\xi_{\rm PEXRIV} \approx 11-32$ for a power law spectrum with $2.19 < \Gamma < 2.43$.

Component	Parameters	REFSCH+DISKLINE	PEXRIV+LAOR	RF
WABS	$N_{\rm H}$ (cm^{-2})	4.0×10^{20} (frozen)	4.0×10^{20} (frozen)	4.0×10^{20} (frozen)
	kT (keV)	0.26 ± 0.01	0.26 ± 0.01	0.27 ± 0.01
ZBREMSS	Redshift	0.026 (frozen)	0.026 (frozen)	0.026 (frozen)
	Norm	$1.86 \pm 0.15 \times 10^{-2}$	$1.78 \pm 0.13 \times 10^{-2}$	$1.08 \pm 0.03 \times 10^{-2}$
	Γ	2.34 ± 0.04	2.43 ± 0.03	2.19 ± 0.02
	$E_{\rm c}$ (keV)	100 (frozen)	100 (frozen)	
Reflection	R	2.0 ± 1.0	1.9 ± 0.5	1.1 ± 0.7
Model	Abundance	1.0 (frozen)	1.0 (frozen)	
	Inclination (°)	30.0 (frozen)	30.0 (frozen)	
	$T_{\rm disk}$ (K)	10^6 (frozen)	10^6 (frozen)	
	ξ (erg cm s^{-1})	66 ± 20	46 ± 38	$14\,200 \pm 4500$
	χ^2_ν	1.15	1.11	1.17

combined these models with a Bremstrahlung soft excess component. The best fit parameters of these combined models are listed in Table 3. Both the PEXRIV and REFSCH models have a disk temperature fixed at 10^6 K, a disk inclination angle fixed at 30° and a disk abundance set to the solar value. The power law cut-off energy was set at 100 keV. A slightly better χ^2 is obtained with the PEXRIV model. The inner and outer radii of the relativistic disk are poorly constrained by the REFSCH+DISKLINE model. Not surprisingly, the fit parameters (see Table 3) are otherwise similar for the two models.

One major variable in these reflection models is the ionisation parameter ξ of the slab ($\xi = 4\pi \times F/n$) where F is the incident flux (ergs s^{-1} cm^{-2}) and n is the hydrogen number density of slab (cm^{-3}). Both the PEXRIV and REFSCH models give a best fit ionization parameter $\xi \approx 50$–70 ergs cm s^{-1} corresponding to a reflection of the primary power law component by moderately ionized material. For these small values of the ionization parameter, the reflection should be similar to that of a cold, neutral slab. Hence, a strong emission line at 6.4 keV would be expected which is not observed. One hypothesis is that the line is smeared by Doppler and gravitational effects. Spectral fitting with a relativistic accretion disk Fe line profile (see Sect. 4) indicates a line energy close to 7 keV inconsistent with emission from iron in low states of ionization. An absorption edge at 7.6 keV would also be inconsistent with a reflection model from a cold, neutral slab of material and would require that the upper layers of the disk are highly ionized.

A comparison of the best fit PEXRIV+ZBREMSS parameters (see Table 3) with those obtained using a POWERLW+ZBREMSS model (see Table 2) shows that the use of a reflection model with a high reflection fraction steepens the power law index of the primary component, therefore reducing the apparent soft-excess above the power law component. This effect, however, is small and an important Bremstrahlung component is still required to account for the soft excess contribution. The contribution of the Bremstrahlung component is only reduced by 10% compared to the model without reflection. Hence, we conclude that reflection of the primary power law component by moderately ionized material can only account for about 10% of the soft excess emission.

5.3. Reflection from highly ionized material

The best fit LAOR model to the Fe Kα line indicates that the X-ray emission could arise from material in high ionization states. Since, as shown by Ross et al. (1999), the PEXRIV model is inaccurate as the disc becomes highly ionized, we also fitted the EPIC spectra with the

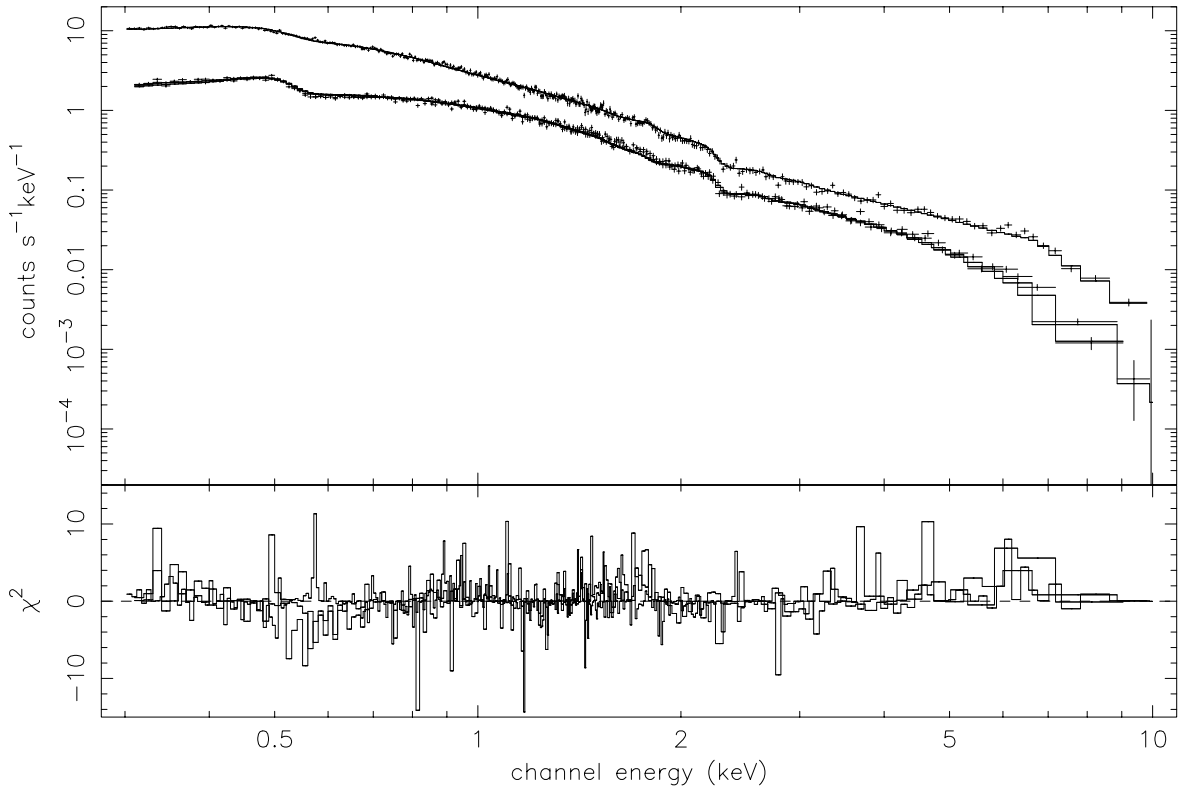

Fig. 5. EPIC p−n (top) and MOS (bottom) spectra compared with the best fit ZBREMSS+RF model to the p−n spectrum (see Table 3). The data and spectral fit are shown in the upper panel. The χ^2 contributions are plotted in the lower panel.

constant density ionised disc models of Ross & Fabian (1993; see also Ballantyne et al. 2001). These models (hereafter called RF models) calculate the spectrum of an input power-law after reflection from an ionized slab. They include lines and edges from Fe, O, Si, Mg, and C and are valid over the energy range 1 eV–100 keV. A larger ionisation parameter, i.e. a more ionized gas, reduces the strength and width of the features in the reflected spectrum including the Fe Kα line and the various absorption edges (Matt et al. 1993, 1996). The computed reflection spectrum is multiplied by a factor R, where R is the reflection fraction, and then added to the illuminating spectrum to produce the model spectrum. Fits with the RF model alone did not provide acceptable results, with a reduced χ^2 of 2.56 for 1297 degrees of freedom. Therefore, as with the PEXRIV models, we combined the RF model with a Bremstrahlung component. The combined model provides an acceptable fit to the data with a reduced χ^2 of 1.17 (see Fig. 5). The fitting parameters are listed in Table 3 and the best fit spectrum is shown in Fig. 7. A comparison of the best fit parameters with those obtained using the PEXRIV or REFSCH model (also Table 3) shows that spectral fitting with the RF model leads to a higher ionization parameter, $\xi \geq 10^4$ erg cm s^{-1} (to be compared with $\xi \approx 10^3$ for PEXRIV using a conversion factor $\xi_{\rm RF}/\xi_{\rm PEXRIV} \approx 20$). A high value of the ionization parameter seems consistent with the best fit LAOR model (see Sect. 4.2) to the Fe K line which suggests that iron is mainly in its highest states of ionization. According to Matt et al. (1993, 1996), only Fe XXV and especially Fe XXVI contribute significantly for $\xi \approx 5000$ erg cm s^{-1}.

The RF model alone cannot account for the entire soft-excess emission. An important Bremstrahlung component is still required in addition to the reflection model to account for the overall soft excess contribution in Mrk 335 spectrum. The temperature of the Bremstrahlung component, $kT = 0.27$ keV is the same as in the previous cases but its normalisation is reduced by ≈50% compared with a simple power law model without reflection. Hence, we conclude that (i) reflection of the primary power law component by highly ionized material is plausible in the nucleus of Mrk 335 but that (ii) reflection from a constant density ionized disk model can only account for 50% of the observed soft excess emission.

In order to explore Comptonisation models, we replaced the Bremstrahlumg model by the COMPTT model (Sunyaev & Titarchuk 1980) thus simulating an accretion disc which outer part is reflective but which inner part is missing and replaced by a hot cloud with no intrinsic reflection. This combined model does not provide an acceptable fit to the Mrk 335 EPIC spectra.

5.4. A hybrid reflection model

One possibility to explain the overall soft-excess contribution is that reflection of the primary powerlaw continuum arises from different regions with material in different states of ionization. For instance, highly ionized material

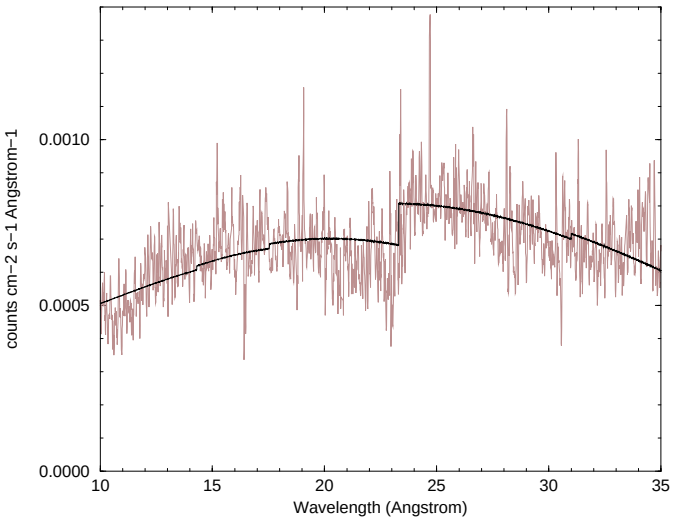

Fig. 6. First order averaged RGS spectrum compared with the best fit phenomenological model consisting of a redshifted power law + Bremstrahlung continuum absorbed by Galactic neutral gas (see Table 2).

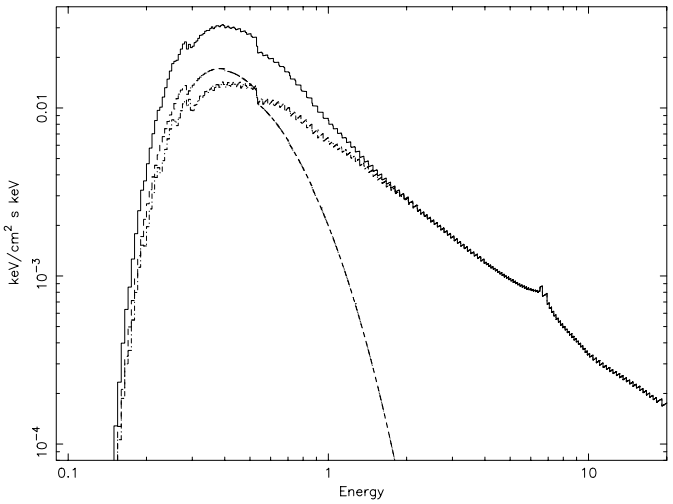

Fig. 7. $F_{\rm E}$ plot of the ZBREMSS+RF spectral model for Mrk 335. The model consisting of a ionized reflector and a Bremstrahlung component is the same as in the count rate spectrum of Fig. 5.

could be present within the inner region of the accretion disk while material in lower states of ionization would be located further out. In order to test this hypothesis, we fitted the EPIC spectra with two RF reflection models. Initial tests were conducted by imposing the same photon index to the primary continuum in both models. Since no acceptable fit was obtained, the photon indices were left free and independent for the two models. In order to determine the ionization parameters which could explain the observed soft excess, we imposed the reflection fractions to be unity for both RF models. Although the parameters are poorly constrained and the fitting accuracy is not acceptable ($\chi^2 = 1.54$) due to residuals below 2 keV, the results are suggestive. The best fit parameters to the combined model suggest a steep power law reflected from moderately ionized material ($\xi \approx 200$ erg cm s^{-1}) and a less steep power law reflected from highly ionized material ($\xi \approx 10^6$ erg cm s^{-1}). The model with the high ionization parameter is the major contributor to the overall spectrum above 6 keV. However, it is an excellent reflector and exhibits negligibly small spectral features resulting from iron. Hence, the iron spectral feature would be produced by moderately ionized material. With $\xi = 100{-}300$ erg cm s^{-1}, the Fe K line emission line could be suppressed because iron in the range Fe XVII – Fe XXIII dominates at the illuminated surface, and its Kα photons are destroyed by the Auger effect during resonance trapping (Ross & Fabian 1993; Zycki & Czerny 1994; Ross et al. 1996). This range of ionization parameters could then explain the existence of an edge at 7.6 keV without the associated presence of an iron K line, thus supporting the single edge phenomenological model (see Sect. 4).

However, one major difference between spectra reflected from midly ($\xi < 10^3$ erg cm s^{-1}) and highly ($\xi > 10^4$ erg cm s^{-1}) ionized material is the presence or absence of emission line features and absorption edges in the soft energy range below 2 keV. Indeed, abundant elements such as oxygen are partially ionized in one case and fully ionized in the other. The high spectral resolution of the RGS spectrometers on board XMM−Newton is well suited to disentangle emission line features from absorption edges and to detect the presence of an absorber or emitter in the 0.3 to 2.1 keV energy band. The average RGS spectrum (see Fig. 6) of Mrk 335 shows an absorption edge at 0.54 keV consistent with galactic absorption by neutral oxygen. However, no evidence is found for K−shell absorption edges at 0.74 keV (OVII) and 0.87 keV (OVIII) characteristic of the presence of ionized material along the line of sight. We fitted RGS data by the best fit continuum model of EPIC data. A $\chi^2_\nu = 1.11$ was obtained with no residuals indicative of absorption lines from ionized gas, from the He and H-like states of the major elements (e.g. C, N, O, Ne ... etc.). The achieved signal to noise ratio of the RGS and EPIC spectra neither reveals the existence of emission lines that could be expected from a midly ionized reflector. In addition, a soft excess mainly produced by reflection from the outer region of an accretion disk would be difficult to reconciliate with the short time variability which we observed in the 0.3–2 keV band.

6. Discussion

6.1. The accretion disk paradigm

The 0.3–10 keV spectrum of Mrk 335 observed by XMM−Newton shows three intrinsic components, namely a power law primary continuum, a soft-excess and a spectral feature around 6.4 keV. These components, present in many Seyfert 1 galaxies, exhibit important specificities in the case of Mrk 335, i.e. (i) their luminosity is highly variable with large amplitudes ($\Delta L > 5 \times 10^{42}$ erg s^{-1}) on timescales as short as a few ksec, (ii) the power law

component above 2 keV has a photon index $\Gamma = 2.3$ much steeper than that of a "normal" Seyfert 1 galaxy, (iii) the spectral feature observed around 6.0 keV is broad ($EW \approx 1$ keV) and can be fitted by a relativistic emission profile and (iv) the soft excess above the power law rises steeply below 2 keV and represents more than 30% of the intrinsic source luminosity in the 0.3–2 keV band.

The power law X-ray emission of radio-quiet AGNs is likely the result of inverse Compton scattering of low-energy photons by relativistics electrons. The Comptonization process could take place either on thermal electrons in an optically thin corona, on thermal electrons in the innermost part of an accretion disk or on non thermal electrons at the base of a jet like flow. Although the geometry of the region emitting the primary X-ray spectrum is unknown, the general consensus is that the power law component originates from an extended corona in the vicinity of an accretion disk (Haardt & Matt 1993). Within the frame of such a model, the Fe K emission in the spectrum of Mrk 335 and its soft excess emission could be produced by Compton reflection of the primary continuum onto an accretion disk. Possible contribution to these reflection components may come from material within the accretion disk itself (Pounds et al. 1990) or from matter further out (Krolik et al. 1994; Ghisellini et al. 1994). Orbital motion deep in a relativistic gravitational potential seems to be the probable interpretation for many Fe K lines profiles that have been observed to be several tens of thousands of $\mathrm{km\,s^{-1}}$ broad and significantly redshifted (Mushotzky et al. 1995; Tanaka et al. 1995; Page et al. 2001; Wilms et al. 2001). Hence, a candidate scenario which could simultaneously account for the broad emission feature and the soft-excess component in Mrk 335 spectrum is a reflection model from highly ionized material in the innermost region of an accretion disk.

However, reflection models from ionized disk model account at most for 50% of the entire soft-excess contribution in the X-ray spectrum of Mrk 335 below 2 keV. Also, a straightforward interpretation of the emission feature around 6.0 keV as a relativistiv Fe K line profile gives an abnormally large equivalent width (>800 eV). These aspects are addressed in the following sections.

6.2. The soft excess contribution

The high signal to noise ratio of our data allows us to characterize the soft X-ray excess contribution with a high confidence level. Confidence in the results is reinforced by the consistent parameters obtained from the simultaneous analysis of the MOS and p−n data. Our analysis concludes that, at the time of the observation, 50% of the soft excess can be accounted by a reflection model from highly ionized material with a constant density. The other 50% contribution can be parametrized by a Bremstrahlung model with a temperature $T = 0.27 \pm 0.01$ keV. In the low energy domain below 2 keV, we did not find evidence for the presence of emission lines or absorption edges other than the edge produced by galactic neutral oxygen.

Explanations for a spectral steepening in the soft X-ray band based on reflection by ionized media have been successfully applied to a few AGNs (Zycki et al. 1994; Piro et al. 1997). According to these scenarii, the inner region of the disk could be photo-ionized by X-rays emitted from the primary continuum source. If the ionization level is such that light elements (such as He, C or O which are the main contributors to photoelectric absorption at low energies) are fully or nearly stripped of electrons, the medium becomes reflective by Thomson scattering of X-rays. In this instance, the soft X-ray excess would be the low energy equivalent of the high energy bump (Czerny & Zycki 1994). The key quantity in determining the ionization state is the ionization parameter ξ. Spectral fitting of the Mrk 335 spectra with the RF model points to an ionization parameter greater than 10^4 $\mathrm{erg\,cm\,s^{-1}}$ implying that the material responsible for the soft X-ray emission is highly ionized and reflective to soft X-rays, thus leading to further enhancement of the soft X-ray excess. For ionization parameters lower than 10^3 $\mathrm{erg\,cm\,s^{-1}}$, detailed models of this reflected component typically include line emission from O VIII ($E = 0.65$ keV) and O VII ($E = 0.57$ keV), with an equivalent width depending on the ionization parameter. The absence of such emission features around 0.6 keV in the RGS spectra of Mrk 335 supports the conclusion derived from the analysis of EPIC data that the reflecting material is highly ionized.

Illumination of a cold disk by hard X-rays leads to the formation of a very hot, optically thin layer of material above the disk (Krolik et al. 1981). The two layers are in pressure equilibrium and the discontinuity in temperature and density reflects the discontinuity in cooling mechanisms. In the hot layer, Comptonization and bremstrahlung play the main roles, but closer to the cool, dense disc, atomic absorption and emission become the major cooling processes. Simulations of spectra resulting from such a model (Ross et al. 1999) indicate that reflection effects of the primary continuum can be largely enhanced below 1.5 keV owing to Bremsstrahlung emission by the hot surface layer and "inverse Compton" upscattering of even softer photons. Depending on the hardness of the primary spectrum, the ionization parameter and the disk density, the temperature of the illuminated surface is found to be extremely high ($T > 10^7$ K) for constant density disk models. It is worth noting that a high but somewhat lower temperature ($T \approx 3 \times 10^6$ K) is suggested by the Bremstrahlung component of the best fit models to the spectrum of Mrk 335. These temperatures indicate that the density structure of the illuminated gas can hardly be uniform with depth. The heating of the uppermost layer by the impinging radiation should result in a density decrease in the upper boundary layer.

Recently, Nayakshin et al. (1900) presented ionized reflection models where hydrostatic equilibrium is solved along with the ionization and radiation structure. They found that, due to a thermal instability, only a very thin

layer with a Thomson depth $\tau \leq 1$ at the top of the slab is highly ionized, and that the reflection spectrum is dominated by the cool neutral material underneath. For $\Gamma < 2$, the equivalent width of the Fe features decreases monotonically with the magnitude of the illuminating flux while the energy centroid of the Fe K line remains at 6.4 keV. For hard X-ray spectra and large X-ray fluxes, the thermal instability forbids the illuminated layers from attaining temperatures between 200 eV and a few keV. Layers with temperatures lower than 200 eV occupy a small Thomson depth and thus contribute little to the reflected spectra. Remarkably, this model is a good description of the ASCA spectrum of Mrk 335 observed in December 1993 and analysed by Ballantyne et al. (2001). Indeed, their best fit RF model indicates a large reflection fraction ($R = 0.68$) and a $\Gamma = 1.98 \pm 0.02$ power law. Consistently with Nayakshin model, their best Gaussian fit to the Fe K line gives a narrow feature ($EW = 189$ eV) at an energy (6.43 keV) corresponding to emission from iron in low states of ionization.

During the XMM−Newton observation in December 2000, the primary power law continuum of Mrk 335 was softer with a photon index $\Gamma = 2.19 \pm 0.02$. The models of Nayakshin et al. (1900) predict that if the disc is radiation pressure dominated and the illuminating power law has $\Gamma \geq 2$, then the previously unstable temperature region between ≈200 eV and 1 keV can become thermally stable not only due to an incident soft X-ray spectrum but also due to a large UV flux. The Compton temperature even at the top of the reflection layer can be lower than 1 keV which can lead to the appearance of highly ionized iron lines in the reflection spectrum if the layer is somewhat optically thick. Hence, X-ray reprocessing calculations that include hydrostatic balance could explain the simultaneous presence of a steep power law, a soft excess component with a Bremstrahlung temperature $kT = 0.26$ keV and the signature of the highest ionization stages of iron in the spectrum of Mrk 335. Reprocessing models that include hydrostatic balance predict that for a steep power law the hot Compton layer becomes visible. Such models could make a noticeable difference in interpretating the spectra of Mrk 335 and other NLS1 galaxies which reveal unusual ionization states (Comastri et al. 1998; Bautista & Titarchuk 1999).

Even if the good fit obtained with the RF model and the presence of a strong iron line suggest that reprocessing is occuring at a significant level, it appears that the strong soft component is not due only to disk reprocessing. The influence of the soft radiation from the disk itself may play an important role (Zheng et al. 1995). The reprocessing scenario described above neglects any intrinsic emission from viscous dissipation in the accretion disk itself. This neglect would not be valid in case the disk accretion rate approaches the Eddington limit as suggested by the large value $\xi \approx 10^4$ of the ionization parameter obtained with the RF model. Hence, it is possible that in December 2000 Mrk 335 was in a situation where accretion was occuring at a high rate and that both reflection from the ionized material in the inner region of the accretion disk and thermal emission produced by the viscous heating of the disk significantly contributed to the soft excess. A soft X-ray component much stronger than expected from a reprocessing origin alone could lead to a strong Compton cooling of the hot electrons responsible for the primary power law continuum. As proposed for the NLS1 galaxies RE 1034+39 (Pounds et al. 1995) and Ton S 180 (Comastri et al. 1998), this could explain the steep tail in the Mrk 335 spectrum above 2 keV if a significant fraction of the gravitational energy is dissipated in the disk phase. Within such a scenario, the soft radiation from the disk itself may contribute significantly to the photoionization of most ionic species, so that an ionization parameter defined solely in terms of the illuminating flux could no longer describe completely the state of the gas. Additional complications in interpreting the observations could arise since part of the emitting and reprocessing material might be relativistic and located within a deep gravitational potential.

6.3. The Fe K line

The broad spectral feature around 6.4 keV in the spectrum of Mrk 335 can be fitted by the relativistic DISKLINE (Fabian et al. 1989) and LAOR (Laor 1991) line models. Such line profiles are expected from the inner part of a disk orbiting either a Schwarschild or a Kerr black hole. The best constraint on the extent of the emitting region is provided by the LAOR model with an inner radius of ≈4 in $\mathrm{GM/c^2}$ units. The line shape and skewness would be due to the combined action of Doppler shifts and gravitational redshifts from matter moving in a disk assumed to be inclined at about 30° from the line of sight. The standard model of emission from iron fluorescence around black holes assumes that there is no fluorescence and almost no material within a radius of marginal stability R_{ms}. R_{ms} is smaller for rotating (Kerr) holes ($R_{\mathrm{ms}} < 6\ \mathrm{GM/c^2}$) than for non-rotating ones. It decreases monotically as the spin of the hole increases. Under the assumption that all iron fluorescence occurs outside R_{ms}, the very broad red wing of the iron line in Mrk 335 rather suggests a Kerr geometry to make the relativistic effect sufficiently strong for emission to be observed below 5 keV. A similar claim for the detection of a Kerr profile in the *XMM–Newton* spectrum of MCG-6-30-25 has been recently made by Wilms et al. (2001). Within the frame of a reflection model, photoionization by the strong radiation field near the black hole would be the dominant process determining the ionization state of the inner disk material in the nucleus of Mrk 335. Fluorescent line emission has been investigated for a whole range of ionisation parameters (Matt et al. 1993, 1996; Ross et al. 1999). For a slab illuminated by a $\Gamma \geq 2$ spectrum with an ionization parameter $\xi = 10^4\ \mathrm{erg\,cm\,s^{-1}}$ as suggested by the best fit RF model, the reflected spectrum shows spectral features due to iron Kα emission and K-shell absorption

(Ross et al. 1999; Nayakshin et al. 1900). Most of the Kα photons emerge in a broad Comptonized emission feature but a fraction of the Kα photons emerge in Fe XXV and Fe XXVI line cores at 6.7 and 7.0 keV. Consistently, the best fit model to the Fe K line of Mrk 335 indicates a broad emission component close to 7 keV and possibly a narrow line at 6.6 keV, thus corroborating that iron is in the highest states of ionization.

The equivalent width of the iron line can be predicted given the source geometry, the illuminating X-ray spectrum, and the chemical abundances. In the standard case where cold material possesses Morrison & McCammon (1983) cosmic abundances and subtends 2π sr at the X-ray source with an AGN-like spectrum, the EW width is $W = 150$ eV. For a more recent set of cosmic abundances (Anders & Grevesse 1993), the EW increases slightly to 190 eV (Reynolds et al. 1995), primarly due to the increased abundance of iron. The equivalent width of the Fe K line in Mrk 335 is comparatively much larger ($EW \approx 830-970$ eV). Several possible explanations for the strong Fe K line have been proposed. First, the iron may be overabundant (George & Fabian 1991; Reynolds et al. 1995) but extreme iron overabundances (>10 $Z_\odot$) would be required to explain such a strong line. Secondly, the geometry might be such that the reflecting material subtends more than 2 π sr at the X-ray source, which is difficult to reconcile with a disk-corona model. Thirdly, gravitational focussing of the X-ray flux from a source which is at some height above the disk plane can enhance the EW of the line (Martocchia & Matt 1996; Reynolds & Begelman 1997). These relativistic effects are specially important for enhancing the emission from the innermost region of the disk within a few Schwarschild radii from the central black hole and produce very redshifted line emission with observed energies of 4 keV or less. Fourthly, any relative motion between the X-ray source and the accretion disk usually enhances the EW of the iron line through the effect of special relativistic aberration and Doppler shifts (Reynolds & Fabian 1997). These enhancement effects of the line EW are especially important if the X-ray emitting material is moving directly towards the disc.

Although these possibilities cannot be excluded, the large equivalent width of the Fe K line in Mrk 335 spectrum could be mainly related to the fact the reflecting material is in high states of ionization. Matt et al. (1993) computed the properties of the iron Kα line by extending the calculation of photoionized slabs made by Ross & Fabian (1993) to cover a complete accretion disk and to include inclination effects. The increase in the line intensity for $\xi > 1000$ erg cm s^{-1} with respect to the cold case is explained by the greater fluorescent yield of highly ionized iron and by the full ionization of lighter elements which therefore cannot absorb the emitted photons. For an X-ray slab illuminated with a power law $\Gamma = 1.8$ spectrum at $\xi = 2000$ erg cm s^{-1}, Ross & Fabian (1993) calculated a EW value of 580 eV for matter subtending 2π sr. However, at higher values of ξ, the total line intensity decreases because an increasing fraction of iron becomes completely ionized. Matt et al. (1996) have shown that in highly ionized disks, there is a subtantial component of the line flux that suffers multiple Compton scattering and which would also emerge as a very broadened spectral feature. Also, a backscattered continuum will accompany the observed iron line emission, and this continuum will have iron K-shell photoelectric edges imprinted into it. The large spread in redshift that contributes to these reprocessing effects results in a smearing of the edges into broad throughs (Ross et al. 1996). Thus, the net continuum that underlies the Fe line in Mrk 335 will possess these features at some level. Since the best fit parameters to the line have been derived from the data assuming a powerlaw continuum with no such smeared edges, the equivalent width of the emission-line profile may differ subtantially from that given in Table 1. In order to assess the importance of such an effect, we fitted the broad emission feature around 6 keV with a LAOR model using the continuum description provided by the best fit RF model (see Table 3). The best fit parameters to the relativistic line model are given in Table 4. A comparison with the LAOR model assuming a power law continuum (see Table 1) clearly demonstrates the large impact of the continuum determination on the equivalent width derivation. It is worth noting that the line equivalent width is significantly smaller ($EW \approx 370$ eV) but that the best fit disk parameters are otherwise very similar.

The ZBREMSS+RF+LAOR fit simulates a scenario where reflection from ionized material in an accretion disk and intrinsic emission from the accreting material in the innermost ($R < 8\ GM/c^2$) region of the disk both contribute to the X-ray spectrum of Mrk 335. The good quality of fit suggests that the Fe K feature could be dominated by the intrinsic emission from the accreting material itself. Within a bulk motion Comptonization model for accretion into a black hole, Bautista & Titarchuk (1999) found that strong Fe XXVI Lyα emission could be formed by resonance fluorescence resulting from the strong radiation field in the region near the black hole, or possibly in the interphase between a hot corona and the optically thick disk. Alternatively, a strong line could be formed by collisional excitation in an accretion flow dominated by advection or gravitational accretion flows with strong shocks. Bautista & Titarchuk (1999) emphasize that fluorescent excitation is very efficient when the continuum flux is sufficiently strong at the energy of Fe XXVI, and when the temperature of the plasma is too low (<few keV) for efficient collisional excitation.

6.4. A candidate scenario

The luminosity of Mrk 335 was highly variable during the *XMM-Newton* observation in December 2000. Erratic count rate fluctuations with low amplitudes and short timescales were superimposed on a steady flux increase. Luminosity variations on timescale as short of a few ksec can be expected from X-ray emitting material orbiting

Table 4. Best fit parameters to Mrk 335 Fe K line assuming emission from a relativistic accretion disc described by the LAOR model with a power law dependence $R^{-\beta}$ of the emissivity. The continuum is described by the best fit RF model (see Table 3).

Model parameters		
Line energy (keV)	7.5 ± 0.3	7.5 ± 0.2
Line equivalent width (keV)	0.390	0.350
β	2 (frozen)	3 (frozen)
Inner radius (units of GM/c^2)	3.3 ± 0.8	3.3 ± 0.6
Outer radius (units of GM/c^2)	6.4 ± 1.2	6.3 ± 0.7
Disk inclination (°)	30 (frozen)	30 (frozen)
Line norm. (ph cm^{-2} s^{-1})	$3.0 \pm 1.2 \times 10^{-5}$	$3.0 \pm 1.5 \times 10^{-5}$
χ^2_ν	0.96	0.96

a $M \approx 10^7\ M_\odot$ blackhole (Zheng et al. 1995) down to 4–12 GM/c^2 radii. Our analysis of the EPIC and RGS spectra of Mrk 335 suggests a scenario where reflection from the ionized material in the inner region of the accretion disk and thermal emission produced by the viscous heating of the disk each contribute to 50% of the soft excess emission. The spectral contribution from the accretion disk itself is described by a Bremstrahlung component with $kT = 0.27$ keV and a total flux $F_{>0.15\ \mathrm{keV}} = 10^{-11}$ erg cm^{-2} s^{-1} above 0.15 keV. This value can be compared with self-consistent calculations (Ross et al. 1992) of the spectra emitted by radiation-pressure dominated regions of standard α accretion disks (Shakura & Sunyaev 1973). For a black hole mass $M = 10^7\ M_\odot$, the flux above 0.15 keV for a face-on accretion disk at the distance of Mrk 335 is estimated to 11×10^{-11} erg cm^{-2} s^{-1} and 2.6×10^{-11} erg cm^{-2} s^{-1} for accretion rates constrained to $L/L_{\mathrm{edd}} = 1/3$ and 1/6 respectively (Ross et al. 1992), where L_{edd} is the luminosity in the Eddington limit. Hence, 50% of the soft excess luminosity in Mrk 335 could be explained by thermal emission from a disk accreting at a rate constrained to about 13% of the Eddington luminosity onto a central object with a mass of $10^7\ M_\odot$. The other 50% of the soft excess luminosity would result from the reprocessing onto the disk of a power law continuum produced by inverse Compton scattering of UV photons within a corona above the disk. This illuminating hard flux, hence the ionization parameter, in the upper layer of the disk would be provided ultimately by accretion also. Ross et al. (1993) noted that value of $\xi \approx 10^4$ erg cm s^{-1} as derived from the best fit RF model to the data appear to imply an accretion rate which is also close to the Eddington limit for a standard accretion disk (Ross & Fabian 1993). This argues for the consistency of our proposed scenario. However, estimate of the accretion rate from the ionization parameter does not take into account the non-uniform density of the disk in its outer few Thomson depths and assumes a continuous corona illuminating the disk with a "normal" hard power law spectrum ($\Gamma = 1.8$). The power law of Mrk 335 is steeper ($\Gamma = 2.3$). Within the proposed model, this results from the cooling of hot electrons by the soft X-ray photons emitted in the inner part of the disk and passing through the extended corona.

A model of an accretion disk with a hot corona also provides a simple explanation for the light curve of Mrk 335. The large amplitude and long timescale variation of the luminosity would be produced in the optically thin corona which could extend in radial directions up to a large distance from the black hole. However, since the soft excess emission from the disk is negligible above 2 keV (see Fig. 7), such a scenario does not explain that count rate variations at high frequencies are also present in the 2–10 keV band and are correlated with the countrate fluctuations in the 0.3–2 keV band (see Figs. 1 and 2). If these rapid luminosity variations are produced in the inner region of the disk, the accretion flow in these regions is in a configuration different from the "standard" accretion disk model developed by Shakura & Sunyaev (1973). Such models derive the accretion flow structure in the limit when the gravitational energy released is radiated locally in a geometrically thin disk and are unable to explain the presence of X-ray emission at high energy.

A solution has been proposed which explains hard and faint X-ray spectra seen from black hole candidates in quiescence (Narayan et al. 1996). Below a critical accretion rate, a stable, hot, optically thin, geometrically thick solution can be found if radial energy transport (advection) is included. In the absence of an optically thick disk, the hot electrons can only cool by Bremstrahlung and the lack of soft photons in these models means that the X-ray spectra are typically hard. Since the geometrically thin disk in Mrk 335 seems to truncate above 3–4 GM/c^2 (see Table 1), this would imply that inside this transition radius the accretion changes to a hot optically thin, geometrically thick flow, plausibly an advection-dominated accretion flow. Such a scenario is consistent with the expectation that disk accretion changes dramatically as the accreting matter reaches the vicinity of the marginally stable orbit. Pushed by gravity and the outer pressure, the gas plunges inward through the event horizon in a time of a few GM/c^3 in the fluid frame (a few minutes for $M \approx 10^7\ M_\odot$). There is no time for slow dissipative processes to heat the gas and for slow cooling processes to remove heat by creating photons (Krolik 1999). Nonetheless, the outgoing radiation still interacts with the electrons responsible for the radiation. In a spherical geometry the competition between light crossing time and Thomson diffusion leads to the

Table 5. Best fit reflection models (Ross & Fabian 1993) to Mrk 335 spectra. The best fit model to the 1993 ASCA data (Ballantyne et al. 1999) is provided for comparison. The best fit parameters to the XMM−Newton data have been derived from a simultaneous fit to EPIC spectra extracted during the first 24 ksec (low flux) and the last 10 ksec (high flux) of the observation (see Fig. 1).

Component	Parameters	ASCA (1993)	XMM Low flux	XMM High flux
	kT (keV)		0.27	0.26
ZBREMSS	Redshift		0.026 (frozen)	0.026 (frozen)
	Norm	0	$0.75 \pm 0.07 \times 10^{-2}$	1.09 ± 10^{-2}
	Γ	1.98 ± 0.02	2.18 ± 0.03	2.24 ± 0.16
RF	R	$0.68^{+0.2}_{-0.1}$	1.0 ± 0.8	1.1 ± 0.8
	$\log(\xi)$ (erg cm s^{-1})	$3.34^{+0.06}_{-0.07}$	4.1 ± 0.3	4.1 ± 0.3
	Reduced χ^2_ν	1.09	1.00	1.07

limit $\Delta L/\Delta t = 2\eta \times 10^{42}$ erg s^{-2} (Guilbert et al. 1983), where η is the conversion efficiency from matter to energy. In the most dramatic luminosity variation of Mrk 335 (see Sect. 3), we measured $\Delta L/\Delta t \approx 5 \times 10^{39}$ erg s^{-2} corresponding to $\eta \approx 0.25\%$. Such a radiative efficiency is much smaller than the nominal 6–42% expected from accretion onto a black hole. The $\eta \approx 0.25\%$ value is consistent with a scenario where the inner region of the disk responsible for the high frequency and low amplitude luminosity variations would be advection-dominated, i.e. most of the dissipated heat is advected inward along with the flow instead of being radiated. Although there could be some contribution to the X-ray emission from within the last stable orbit, it is still not that clear from the theoretical studies in the literature what its exact contribution will be. If most of the dissipated potential energy is retained in the accreting gas as heat, the temperature of the ions must rise. The thin disk model may no longer be appropriate and the dynamics of accretion could become similar to spherical accretion. A rate of accretion constrained to 13% of the Eddington limit would then translate into 1.6×10^{-2} $M_\odot$ yr^{-1}. One model suggested to explain the steep X-ray spectrum of extreme soft X-ray sources, such as NLS1 galaxies, is that these sources accrete at an unusually high rate leading to a large soft photon flux. These photons then Compton cool the hard photon source, generated in a hot accretion disk corona, resulting in a steeper X-ray spectrum (Pounds et al. 1995). The scenario we propose is consistent with this model and predicts that, if the accretion rate and luminosity increase, the thermal emission of the disk (parametrized by the Bremstrahlung component) shall also increase. After some delay, the Comptonization continuum produced in the corona above the disk should become steeper and more intense. The reflection fraction of the illuminating continuum and the ionization parameter should also increase unless the upper layer of the disk is already fully ionized. Analysis of the EPIC spectra of Mrk 335 for two luminosity levels corresponding respectively to the first 24 ksec (low flux) and to the last 10 ksec (high flux) of the EPIC exposure (see Fig. 1) confirms this behavior (see Table 5) since the normalisation factor of the Bremstrahlung component increases with the photon index of the primary continuum. The proposed model also accounts for the fact that the best fit RF model to the ASCA spectrum of Mrk 335 obtained in December 1993 (Ballantyne et al. 2001) did not require an additional Bremstrahlung component and showed a smaller photon index, reflection fraction and ionization parameter (see Table 5). From this comparison, we further conjecture that Mrk 335 might be in a transition between a normal Seyfert 1 state and an ultra-soft NLS1 state (Pounds et al. 1995) where the soft-excess emission is fully dominated by the intrinsic emission from the accreting material.

7. Summary

Changes of luminosity $\Delta L > 5 \times 10^{42}$ erg s^{-1} on size scales smaller than a light hour support the view that gravitational energy conversion linked with the presence of a supermassive object is likely responsible for the X-ray emission from the nucleus of Mrk 335. The best fit parameters to the Fe K line using a relativistic disk line profile point to a scenario where the iron K emission arises from highly ionized material in the innermost region of an accretion disk surrounding a rotating black hole. Our analysis of the X-ray continuum emission of Mrk 335 suggests a scenario where both reflection from highly ionized material in the inner region of the accretion disk and thermal emission produced by the viscous heating of the disk itself contribute to the soft excess. Half of the soft excess luminosity in Mrk 335 spectrum could be explained by thermal emission from a disk accreting onto a 10^7 $M_\odot$ central object at a rate constrained to about 13% of the Eddington luminosity. The remaining 50% of the soft excess luminosity would result from the reprocessing onto the disk of a power law continuum produced by inverse Compton scattering of UV photons within a corona above the disk. The inner region of the disk responsible for the high frequency and low amplitude luminosity variations could be advection-dominated with a radiation efficiency as low as 0.25%. The disk may no longer be thin in this inner region and the dynamics of accretion could become similar to spherical accretion. A rate of accretion constrained to 13% of the Eddington limit would then translate into 1.6×10^{-2} $M_\odot$ yr^{-1}. We further conjecture that Mrk 335 might be in a transition between a normal Seyfert 1 state and an ultra-soft NLS1 state where the soft-excess

emission is fully dominated by the intrinsic emission from the accreting material.

Acknowledgements. We thank our colleagues from the *XMM–Newton* Science Operation Centers for their support in implementing the observations. We are grateful to the referee, Dr. J. Reeves, for the improvements suggested to an earlier version of the manuscript.

References

Anders, E., & Grevesse, N. 1989, Geochim. Cosmochim. Acta, 53, 197
Ballantyne, D. R., Iwasawa, K., & Fabian, A. C. 2001, MNRAS, 323, 506
Bao, G., & Ostgaard, E. 1994, ApJ, 422, L51
Bautista, M. A., & Titarchuk, L. 1999, ApJ, 511, 105
Bianchi, S., Matt, G., Haardt, F., et al. 1999, A&A, 376, 77
Boller, Th., Brandt, W. N., & Fink, H. 1996, A&A, 305, 53
Comastri, A., Fiore, F., Guainazzi, M., et al. 1998, A&A, 333, 31
Czerny, B., & Zycki, P. T. 1994, ApJ, 431, L5
Edelson, R. A., & Malkan, M. A. 1986, ApJ, 308, 59
Fabian, A. C, Rees, M. J., Stella, L., et al. 1989, MNRAS, 238, 729
George, I. M., & Fabian, A. C. 1991, MNRAS, 249, 352
George, I. M., Turner, T. J., Netzer, H., et al. 1998, ApJS, 114, 73
Ghisellini, G., Haardt, F., & Matt, G. 1994, MNRAS, 267, 743
Gondoin, P., Aschenbach, B., Erd, C., et al. 2000, SPIE Proc., 4140, 1
Gondoin, P., Lumb, D., Siddiqui, H., et al. 2001a, A&A, 373, 805
Gondoin, P., Barr, P., Lumb, D., et al. 2001b, A&A, 378, 806
Guilbert, P. W., Fabian, A. C., & Rees, M. J. 1983, MNRAS, 205, 593
Haardt, F., & Matt, G. 1993, MNRAS, 261, 346
den Herder, J. W., Brinkman, A. C., Kahn, S. M., et al. 2001, A&A, 365, L7
Jansen, F., Lumb, D., Altieri, B., et al. 2001, A&A, 365, L1
Krolik, J. H., Mc Kee, C. F., & Tarter, C. B. 1981, ApJ, 249, 422
Krolik, J. H., Madau, P., & Zycki, P. 1994, ApJ, 420, L57
Krolik, J. H. 1999, in Active Galactic Nuclei: From the Central Black Hole to the Galacatic Environment, Princeton Series in Astrophysiscs, ed. J. P. Ostriker, & D. N. Spergel (Princeton, New Jersey)
Laor, A. 1991 ApJ, 376, 90
Leighly, K. 1999, ApJS, 125, 317
Magdziarz, P., & Zdziarski, A. A. 1995, MNRAS, 273, 837
Martocchia, A., & Matt, G. 1996, MNRAS, 282, L53
Matt, G., Fabian, A. C., & Ross, R. R. 1993, MNRAS, 262, 179
Matt, G., Fabian, A. C., & Ross, R. R. 1996, MNRAS, 278, 1111
Morrison, T., & McCammon, D. 1983, ApJ, 270, 119
Mushotzky, R. F., Fabian, A. C., Iwasawa K., et al. 1995, MNRAS, 272, L9
Nandra, K., & Pounds, K. A. 1994, MNRAS, 268, 405
Narayan, R., McClintock, J. E., & Yi, I. 1996, ApJ, 457, 821
Nayakshin, S., Kazanas, D., & Kallman, T. R. 2000, ApJ, 537, 833
Page, M. J., Mason, K. O., Carrera, F. J., et al. 2001, A&A, 365, L152
Piro, L., Balucinska-Church, M., Fink, H., et al. 1997, A&A, 319, 74
Pounds, K. A., Stanger, V. J., Turner, T. J., et al. 1987, MNRAS, 224, 443
Pounds, K. A., Nandra, K., Stewart, G. C., et al. 1990, Nature, 344, 132
Pounds, K. A., Done, C., & Osborne, J. P. 1995, MNRAS, 277, L5
Reynolds, C. S., Fabian, A. C., & Inoue, H. 1995, MNRAS, 276, 1311
Reynolds, C. S., & Begelman, M. C. 1997, ApJ, 488, 109
Reynolds, C. S., & Fabian, A. C. 1997, MNRAS, 290, L1
Reynolds, C. S. 1997, MNRAS, 286, 513
Ross, R. R., Fabian, A. C., & Mineshige, S. 1992, MNRAS, 258, 189
Ross, R. R., & Fabian, A. C. 1993, MNRAS, 261, 74
Ross, R. R., Fabian, A. C., & Brandt, W. N. 1996, MNRAS, 278, 1082
Ross, R. R., Fabian, A. C., & Young, A. J. 1999, MNRAS, 306, 461
Shakura, N. I., & Sunyaev, R. A. 1973, A&A, 24, 337
Stark, A. A., Gammie, C. F., Wilson, R. W., et al. 1992, ApJS, 79, 77
Stella, L. 1990, Nature, 344, 747
Strüder, L., Briel, U., Dennerl, K., et al. 2001, A&A, 365, L18
Sun, W. H., & Malkan, M. A. 1978, ApJ, 346, 68
Suniaev, R. A., & Titarchuk, L. G. 1980, A&A, 86, 121
Tanaka, Y., Nandra, K., & Fabian, A. C. 1995, Nature, 375, 659
Tananbaum, H., Peters, G., Forman, W., et al. 1978, ApJ, 223, 74
Turner, T. J., & Pounds, K. A. 1988, MNRAS, 232, 463
Turner, T. J., George, I. M., & Mushotzky, R. F. 1993, ApJ, 412, 72
Turner, T. J., George, I. M., & Nandra, K. 1998, ApJ, 508, 648
Turner, M. J. L. T., Abbey, A., Arnaud, M., et al. 2001, A&A, 365, L27
Vaughan, S., Pounds, K. A., Reeves, J., et al. 1999, MNRAS, 308, L34
Wang, T., Brinkmann, W., & Bergeron, J., 1996, A&A, 309, 81
Wilms, J., Reynolds, C. S., Begelman, M. C., et al. 2001, MNRAS, 328, L27
Zheng, W., Kriss, G. A., Davidsen, A. F., et al. 1995, ApJ, 444, 632
Zycki, P. T., Krolik, J. H., Zdziarski, A. A., et al. 1994, ApJ, 437, 597
Zycki, P. T., & Czerny, B. 1994, MNRAS, 266, 653